Proceedings of the 5th IEEE
International Symposium on Assembly and Task Planning
Besançon, France • July 10-11, 2003

Rotational Force-feedback Wrist

Nicolas Cauche† Alain Delchambre† Patrice Rouiller* Patrick Helmer* Charles Baur* Reymond Clavel*

†Université libre de Bruxelles
CAD/CAM Department
Av F. D. Roosevelt, 50, CP 165/14
B-1050 Brussels, Belgium

* Swiss Federal Institute of Technology (EPFL)
VRAI GROUP, Production and robotic institute
CH-1015 Lausanne
Switzerland

Abstract

Force-feedback structures are mechanical structures that can generate forces to restore to the user a tactile feeling corresponding to the world in which he is manipulating an object. This paper presents the mechanical design of a 3-rotational-degrees-of-freedom (DOF) wrist able to produce force feedback. The wrist, plugged on an existing 3-translation-DOF Delta force-feedback structure (called Delta haptic device), yields a 6-DOF force-feedback structure. The wrist comprises a stylus which is the interface with the user. The kinematic chain of the wrist is serial and composed by a Cardan corresponding to the pitch and the yaw, followed by a rotational joint for the roll. The originality of the wrist comes from the parallel actuation of the Cardan. The advantage of such an actuation is to provide a torque with low inertia and low friction less depending on rotations. The direct geometrical model of the wrist has been implemented, as well as the management of torques and currents applied. Several tests performed show the limit of the actuation of the roll compared with the very promising parallel actuation of the Cardan.

1 Introduction

Objects can be manipulated by humans in the real world (tele-manipulation) as well as in the virtual world (virtual reality). Usually, the systems used to make the interface between human and the world in which he manipulates objects suffer from a lack of tactile feedback. In many applications, it would be useful not only to see what one is doing but also to get some sense of touch information. For example, during an endoscopy, the only feedback the surgeon has is visual (from the endoscopic camera), tactile feedback is non-existent. Force-feedback structures can restore this feeling by generating forces (torques) corresponding to the world in which the object is manipulated.

Force-feedback systems are used in many different domains, such as nanotechnology (nanotube manipulation), medical training or simulation, games, tele-manipulation of robots in hostile environment (Mars, nuclear disaster, sea, etc).

The Delta haptic device structure [1] (figure 1), developed by the VRAI (virtual reality and active interfaces) Group at EPFL (Swiss Federal Institute of Technology, Lausanne, Switzerland), is such a system.

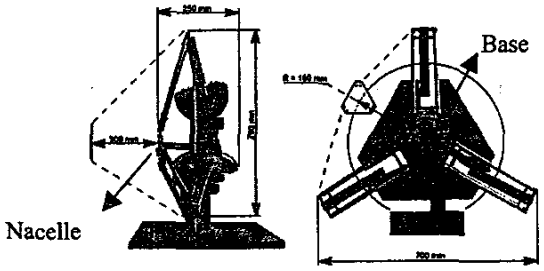

Figure 1: Delta haptic device.

Due to the geometry of the Delta, the nacelle (triangular part linking the parallel arms of the Delta) is mechanically constrained to move with a fixed orientation (always parallel to the base). It is however possible to replace the nacelle by a second structure to obtain a 6-DOF force-feedback structure [2].

The main aim of the research [3] conducting to this paper was to develop a 3-rotational-DOF force-feedback wrist that could be easily plugged on the Delta as a module. A specific application of that wrist is the simulation of a dentist's operation where the stylus represents the surgical tools.

This paper is organised as follows: a state of the art is presented in section 2; section 3 presents the specifications of the wrist and its kinematic structure is presented in section 4; section 5 describes the selected force generation device; the originality of the wrist is presented in section 6 with the parallel actuation of the Cardan, while section 7 presents the geometrical model; finally, performances of the constructed wrist and conclusions are drawn in section 8.

2 State of the Art

Many 6 DOF force-feedback systems already exist. Freedom 6S Haptic device and University of Colorado visual-haptic interface are haptic devices using a stylus interface.

Other more general haptic devices are listed in table 1 with their specifications.

Freedom 6 S Haptic device is commercialised by MPB technology since 1999 [4]. Its kinematical chain consists in a serial arm for the translations and a hybrid (serial and parallel) wrist for the rotations. Its main advantage is that the motors are fixed on the base, which provides a low inertia. Many pulleys and long cables are used to transmit forces between the fixed part and the moving one, leading to high friction. The angular resolution is about 0.29°.

The University of Colorado has developed its own device [5] composed of six actuators each of which actuates a prismatic joint that produces a radial force on rod. The extremity of each rod is linked, three by three, by a spherical joint to the extremities of the stylus. Its advantage is the completely parallel structure that provides a high stiffness compared to serial one. This device is configurable from 3 to 6 DOF.

MagLev is developed at Carnegie Mellon University. Force-feedback is produced with six windings producing six magnetic fields [6].

Hand Controller is a bulky serial haptic device commercialized by Cybernet Corporation [7].

Iwata Haptic Master is a compact haptic device based on parallel structure developed by Dr Iwata at university of Tsukuba. Nine motors are necessary to control the 6 DOF [8].

Laparoscopic Impulse Engine is commercialized by Immersion Corp. for training doctors [2] [9].

PHANToM is a 6 DOF device with a finger interface [10].

Device	DOF	Workspace Y-P	Workspace R	Torque (Nm)	Interface
Freedom 6S	6	100°	320°	0.08 (C) 0.12(I)	stylus
Colorado Uni.	6	120°	-	-	stylus
Iwata Haptic Master	6	-	-	0.55	sphere
Hand control.	6	90°	180°	4.5(I)	handle
MagLev	6	15°-20°		6	handle
Laparoscop impulse engine	3	-	-	0.42	surgical tools
PHANToM	6	Y:335° P:260°	335°	0.18(Y,R;C) 0.05(P;C)	finger
Wrist spec.	6	120°	360°	>0.1(P,Y;C) >0.02(R;C)	stylus

Y: Yaw P: Pitch R: Roll
C: Continuous torque I : Instantaneous torque

Table 1: Haptic device characteristics.

3 Specifications

The overall performances of a force-feedback structure are imposed by human senses [11]. The specifications can be listed as follows:

- The mechanical system should have low inertia, high stiffness with low friction and no force discontinuity.
- The actuators should provide effective and constant torque in the whole workspace.
- Sensors should be precise enough to feel no geometric "steps" in the feedback.
- The overall system should not incommode the user by the volume of the mechanical part, the hotness of the motors and the position of the interface.

After experimentations, it has been established that the torque felt by the user has to be over 0.1Nm for the pitch and the yaw and over 20mNm for the roll.

The workspace will be a cone of 60° for the pitch (rotation ϑ_1 around axis 1) and the yaw (rotation ϑ_2 around axis 2) and 360° for the roll (rotation ϑ_3 around axis 3) (figure 2). The angular resolution required to feel no step in the feedback is fixed at 0.1°.

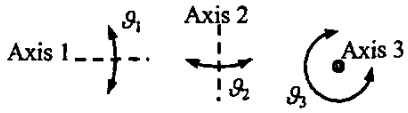

Figure 2: Pitch, yaw and roll.

The wrist will comprise a stylus for the user-interface. Because the wrist is destined to be a module of the Delta haptic device, its weight (< 500g) and volume are limited. The wrist must not interact with the structure of the Delta in its whole workspace.

4 Kinematic Structure of the Wrist

The three rotations can be provided by the following joints and systems: a spherical joint, three rotational joints placed in series, a Cardan and a rotational joint in series or parallel structures.

The authors opted for a Cardan (yaw and pitch) and rotational joint (roll) in series (figure 3), which presents the following advantages: limited dimensions, little number of joints, large workspace, simplicity and concurrences of the axes.

The structure is separated in four frames: the nacelle and three frames (F1, F2, F3) (figure 3). The nacelle is fixed on the Delta haptic device. Frame 1 rotates relatively to the nacelle around axis 1 (A1). Frame 2 rotates relatively to frame 1 around axis 2. Frame 3 is the stylus, which rotates relatively to frame 2 around axis 3 (stylus axis).

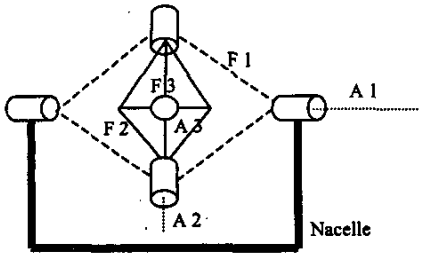

Figure 3: Cardan in series with a rotational joint.

5 Force Generation

Three DC motors are used to generate forces. They are preferably fixed on the nacelle to minimise the inertia. Cables were chosen to link the motor to the different rotational frames, because they are flexible, present a minimal backlash and make the use of a reduction stage possible.

A strained cable linked to the frame at a distance d from the rotation axis allows transmitting a torque to the frame (figure 4a).

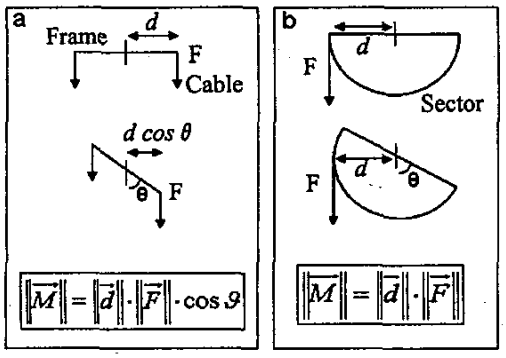

Figure 4: Torque: a) without sector; b) with sector.

Sectors (figure 4b) are used to produce a torque independent of the angular position of the frame.

The major inconvenient of cables is that they can only produce a drawing force and thus a torque only in one sense. To produce an opposite torque without doubling the number of motors, the following solutions are available:

The first system is the "spring versus motor" solution (figure 5). The final torque felt by the user is given by the following equation:

$$M_{\pm} = \left(\frac{R}{r} M_{motor} - K \cdot (X + X_0 - L_0) \cdot R \right) \qquad (1)$$

where R, r are respectively the radius of the sector and the motor pinion, K is the stiffness of the spring, X_0 the prestressed length of the spring, L_0 the free length of the spring, M_{Motor} the torque produced by the motor, X the spring elongation from the prestressed length and M the torque felt by the user.

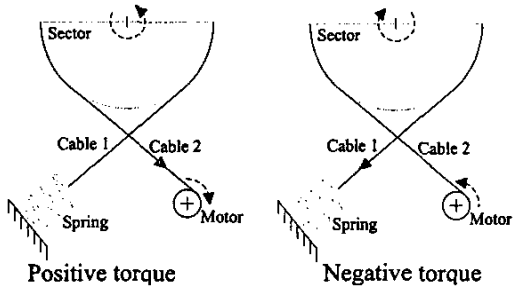

Figure 5: Spring versus motor.

A drawback of this system is that the motor is not used at its maximal capacity because it has to compensate the spring torque. Another inconvenient is that the motor always yields a torque, even if one needs not to feel any. The consumption is thus not optimised and the resulting hotness of the motor can disturb the user. Finally, due to the stiffness of the spring, the maximal produced torque is not equal in each angular position of the frame.

The second system is the "spring versus motor and spring" solution (figure 6).

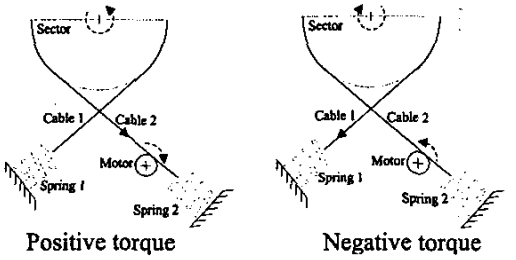

Figure 6: Spring versus motor and spring.

To optimise the effect of the motor torque, a second spring (Spring 2) can be added behind the motor. The final torque felt by the user is given by the following equation:

$$M_{\pm} = \left(\frac{R}{r} M_{motor} + R \cdot K_2 \cdot \Delta_2 - R \cdot K_1 \cdot \Delta_1 \right) \qquad (2)$$

with $\Delta = X + X_0 - L_0$.

When no torque is needed, the motor has only to compensate the difference between torques given by the different springs. Note that the formula is always valid for M_+ but is valid for M_- only if $|M_{Motor}| < r\,K_2\Delta_2$. This is physically understandable because the motor can not help to give a negative torque. The major drawback of this system is that the springs produce a torque depending on the angular position.

The third system is the bi-directional cable system (figure 7). It has the advantage that the motor can transmit a con-

stant torque in the positive and in the negative sense. The final torque felt by the user is given by the following equation:

$$M_{\pm} = \frac{R}{r} M_{motor} \qquad (3)$$

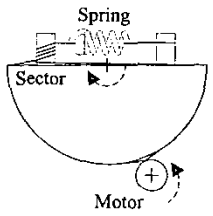

Figure 7: Bi-directional cable system.

The spring is used to strain the cable for assembling and to compensate the backlash in case of cable strain loss. This configuration uses the Cabestan system which makes possible to maintain an important force (strain cable) with a little force (spring force) by enrolling the cable several times on a cylindrical tube.

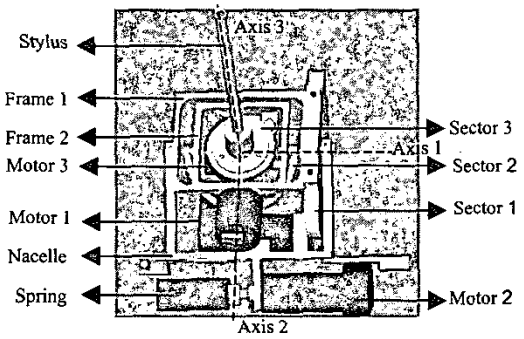

Figure 8: General view of the wrist's implementation.

Each solution has advantages and drawbacks. The necessity to place the motor pinion close to the sector constitutes the disadvantage of the bi-directional cable system. The choice of this system for rotation 2 or 3 will require a motor which will not be placed on the nacelle and will then move with previous rotation in the kinematic chain. This will increase the inertia, which is to be minimised. Its advantage is the constant torque supplied. The "spring versus motor and spring" solution allows placing the motor on the nacelle. Hence, its advantage is the low inertia generated. However, its difficulty consists in finding a path for the cable that does not interact with the wrist structure, especially for rotation 3.

6 Parallel Actuator Structure

Systems available to generate forces for a single rotation were developed in the previous section. In this section, implementation of these systems (figure 8) for the kinematical chain of the wrist will be described focussing on the Cardan.

For rotations of the Cardan, a parallel actuator structure was chosen. It is composed of a bi-directional cable solution for rotation 1 as described in figure 9 and of "a spring versus motor and spring" solution for rotation 2 (figures 9 and 10).

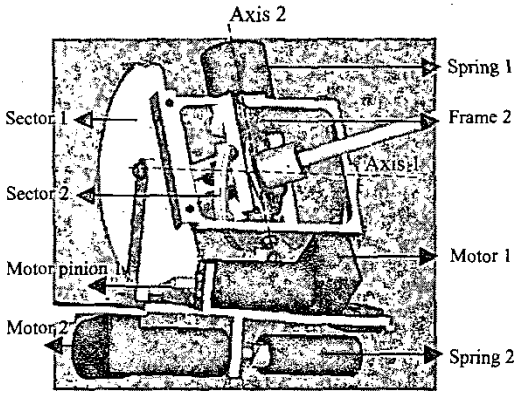

Figure 9: Parallel actuator of rotations 1 and 2.

Implementation of rotation 1 is simple and corresponds exactly to figure 7.

The major problem of actuating rotation 2 with fixed motor was to implement a solution that produces the most constant possible torque for any position of rotation 1 and 2. To provide this with low friction, the cable has to arrive with a fixed orientation to the motor pinion in any configuration of rotations. Sector 2 is mounted on bearings to stay always in a vertical plan (figure 10). This plan rotates around a vertical axis. The cable that follows the sector passes always through the same point, which is the lowest point of sector 2, but with different orientations. A pulley is mounted on bearings along the rotation axis of sector plan. This pulley makes the cable arrive to the motor pinion with always the same orientation. The pulley is oriented by the tension in the cable and is always parallel to sector 2. The cable follows the rotation axis of the sector plan to finally be attached on the motor pinion.

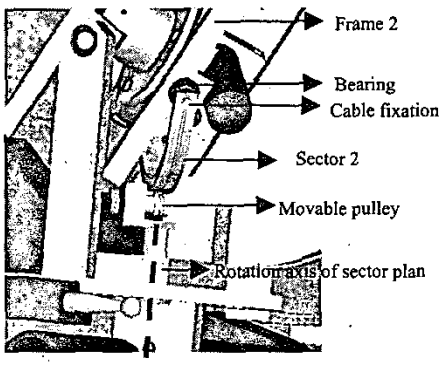

Figure 10: Sector 2 in any configuration.

As said previously, the cable links sector 2 to motor 2 without following the kinematical chain. Torsion springs are

used instead of traction springs because of their excellent stiffness/volume ratio.

For rotation 3 between frame 3 and frame 2, the results of the torque implementation determine a very light motor. This motor can easily be placed just under sector 3 and a bi-directional cable system is then chosen to supply a constant torque. This bi-directional cable system needs intermediary pulleys.

Finally, the following equations are obtained for the overall wrist:

$$M_{\vartheta 1} = \frac{R_1}{r_1} M_{motor} \tag{4}$$

$$M_{\vartheta 2} = K_1 \cdot (\vartheta_2 + \vartheta_{01}) - (K_2 \cdot (\vartheta_2 \cdot \frac{R_2}{r_2} + \vartheta_{02}) - M_{motor}) \cdot \frac{R_2}{r_2} \cdot \cos\vartheta_1 \tag{5}$$

$$M_{\vartheta 3} = \frac{R_3}{r_3} M_{motor} \tag{6}$$

Where $\vartheta_{01}, \vartheta_{02}$ are the prestressed angle of Spring 1 and 2, and ϑ_1, ϑ_2 are the angle of rotation 1 and 2.

Equation (4) and (6) are the bi-directional system equation (3). Equation (5) is composed of the frame torque given by spring 1 minus the frame torque given by spring 2 and the motor.

7 Geometrical Model

The geometrical model (figure 11) of the wrist has been implemented. The angular positions of the frame are calculated from encoders placed on DC motors. The direct geometrical model transforms the angles from the motor reference axis (ϑ_{mot1}, ϑ_{mot2}, ϑ_{mot3}) to the mechanical reference axes (ϑ_1, ϑ_2, ϑ_3) and finally to the reference axis (α, β, γ) used in the virtual reality by the following equations:

$$\alpha = \vartheta_1 = \frac{r_1}{R_1} \cdot \vartheta_{mot1} \tag{7}$$

$$\beta = \vartheta_2 = \frac{r_2}{R_2} \cdot \vartheta_{mot2} \tag{8}$$

$$\gamma = \vartheta_3 = \frac{r_3}{R_3} \cdot \vartheta_{mot3} \tag{9}$$

Each angular position array corresponds to a torque array given by the virtual reality. The inverse torque model transforms the torque array from the virtual reference system to the mechanical reference system and corresponding currents are produced by DC motors. This is calculated by using successively equation (10), inverse of (4–6) and (11).

$$\begin{pmatrix} M_{\vartheta 1} \\ M_{\vartheta 2} \\ M_{\vartheta 3} \end{pmatrix} = \begin{pmatrix} -c\vartheta_1 \cdot tg\vartheta_2 & s\vartheta_1 \cdot tg\vartheta_2 & 1 \\ s\vartheta_1 & c\vartheta_1 & 0 \\ c\vartheta_1 / c\vartheta_2 & -s\vartheta_1 / c\vartheta_2 & 0 \end{pmatrix} \cdot \begin{pmatrix} M\alpha \\ M\beta \\ M\gamma \end{pmatrix} \tag{10}$$

$$I_{mot} = \frac{1}{Cc} \cdot M_{motor} \tag{11}$$

If the required torque array cannot be obtained with the DC motors, the algorithm maintains the orientation of the array but the norm of the torque is decreased.

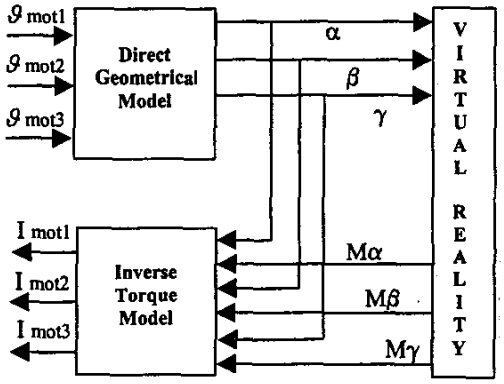

Figure 11: Geometrical model.

8 Results and Conclusion

The final performances of the constructed wrist (table 2) are generally better than the specifications, two features excepted: the weight and the resolution of rotation 3.

Caract \ Rot	ϑ_1	ϑ_2	ϑ_3
Workspace	60° cone		+/- 180°
Max. Torque (Nm)	518	100-550	22
Resolution	0.01°	0.015°	0.78°
Weight	930g		

Table 2: Characteristics of the constructed wrist.

The originality of this wrist lies in its parallel actuator structure that provides, with fixed motors, torques most constant possible of the angular position of the frames. However, it is not possible to obtain strictly constant torques. The maximal positive and negative torque for rotation 2 calculated with equation (5) is represented in figure 12 and 13.

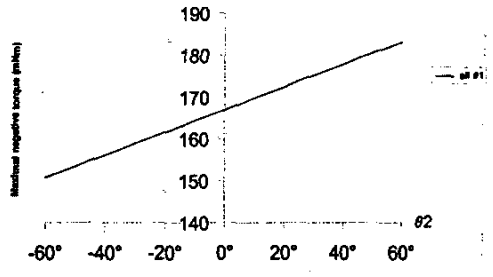

Figure 12: Maximal negative torque versus ϑ_2.

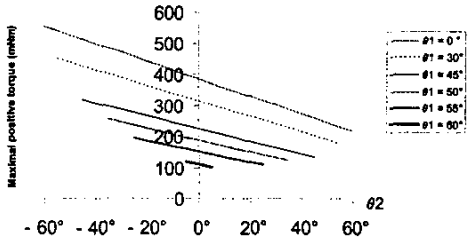

Figure 13: Maximal positive torque versus θ_2.

The variation can be decreased by choosing springs with lower stiffness.

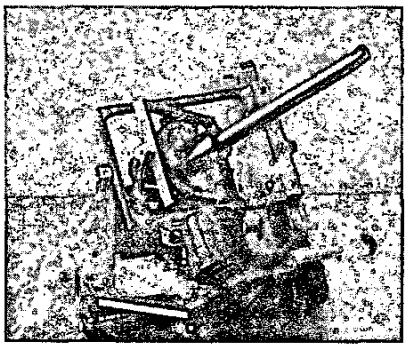

Figure 14: The rotational wrist realised.

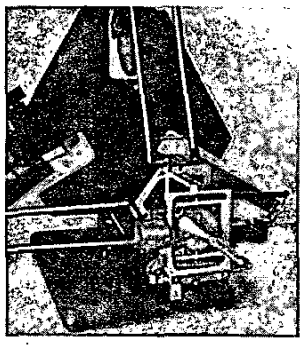

Figure 15: Six DOF force feedback structure.

Tests performed confirm the choice of the kinematic chain and the dynamic system used for the Cardan. In fact, the torque-feedback of rotation 1 is nearly perfect and no friction can be felt. Rotation 2 is less effective for the torque-feedback and friction is higher. Rotation 3 is really depending on the tension in the cable obtained by the spring of the Cabestan system. On the one hand, a highly strained cable provides too much friction and the torque-feedback becomes merely non-existent. On the other hand, a cable with little tension provides nearly no friction, which results in unwanted sliding on the motor pinion. If an acceptable compromise cannot be found, the dynamic system for rotation 3 has to be changed, for example by using a "spring versus motor and spring" system or by another configuration of the bi-directional cable system.

In the future, the parallel actuation system will certainly be kept but the actuation system of rotation 3 will probably be changed to obtain a performing device. In the same way, effort has to be made to miniaturise the overall wrist and thus reduce its weight.

On figure 14 one can see the wrist realised, which provides the three rotational DOF force feedback. Plugged on the Delta haptic device, it yields a 6-DOF force-feedback structure shown in figure 15.

References

[1] S. Grange, C. Baur, "The Delta haptic device," Mecatronics, Besançon, France, 2001.

[2] P. Helmer, *3D force-feedback wrist,* MS thesis, Swiss Federal Institute of Technology, Lausanne, Switzerland, 2000.

[3] N. Cauche, "Réalisation d'un système à retour de force à grande course," Travail de fin d'études, ULB-EPFL, Lausanne, Switzerland, 2002.

[4] MPB Technologies. Freedom 6 S Force Feedback Hand Controller. [Online] Available: www.mpb-technologies.ca [15 January 2003].

[5] C.D. Lee, D.A. Lawrence, L.Y. Pao, "Guaranteed Convergence rates for five degree of freedom in-parallel haptic interface kinematics," *IEEE Conference on robotics and automation,* vol.4, pp. 3267-3274, 1999.

[6] P.J. Berkelman, Z.J. Butler, R.L. Hollis, "Design of a hemispherical Magnetic Levitation Haptic Interface Device," *ASME IMECE*, vol.58, pp 483-488, 1996.

[7] Jacobus et al. U.S. Patent 5,629,594 *"Force feedback system,"* Cybernet Systems Corp., 1997.

[8] H. Iwata, "Artificial Reality with Force-feedback: Development of Desktop Virtual Space with Compact Master Manipulator," *Computer Graphics,* vol.24, no.4, pp. 165-170, 1990.

[9] R. Baumann, *Haptic interface for virtual reality based laparoscopic surgery training environment,* Ph.D.Thesis, Swiss Federal Institute of Technology, Lausanne,Switzerland, 1997.

[10] T. Massie, M Stanley,J.E. Colgate, "PHANToM haptic interface: a device for probing virtual objects," *Dynamic Systems and Control, ASME*, New York, 1994. pp. 295-299.

[11] S. Grange, C Baur, C., "The Delta haptic device as a nanomanipulator," *SPIE Microrobotics and microassembly III*, Boston, MA, November 2001.